A Letters Journal Exploring the Frontiers of Physics

August 2024

EPL, **147** (2024) 35003
doi: 10.1209/0295-5075/ad5e1c

www.epljournal.org

Enhanced optical pumping using mutually orthogonal magnetic fields for quantum sensing

Sudip Mandal[1], Raghwinder Singh Grewal[2] and Swarupananda Pradhan[1,3(a)]

[1] *Photonics and Quantum Optics Section, Atomic and Molecular Physics Division, Bhabha Atomic Research Centre Facility - Visakhapatnam-531011, India*
[2] *Division of Mathematical and Physical Sciences, School of Arts and Sciences, Ahmedabad University Commerce Six Roads, Navrangpura, Ahmedabad-380009, India*
[3] *Homi Bhabha National Institute, Department of Atomic Energy - Mumbai-400094, India*

received 22 April 2024; accepted in final form 2 July 2024
published online 22 August 2024

Abstract – The atomic population trapped in irrelevant atomic states is a limiting factor for sensors based on laser-atom interaction. Using a bi-chromatic light field along with a specific combination of magnetic fields, we show a significant increase in the amplitude (*i.e.*, more than seven times) of a two-photon coherent population trapping (CPT) resonance, which can be effectively used for atomic magnetometry. This increase in amplitude can be explained through enhanced optical pumping via the transfer of population to the relevant Zeeman states. Our experimental observations are consistent with the theoretical calculations carried out for a realistic three-level atomic system using density matrix formalism. We further discuss the optimum condition for enhanced optical pumping by adjusting the ground-state decoherence rate. Enhanced optical pumping through the manipulation of the magnetic field is quite important and is of great interest in the field of quantum technology.

The efficient quantum state engineering is the basis of many atom-based quantum technologies, such as quantum computation, quantum sensors, and quantum communication [1–3]. The pursued methodology has been instrumental in testing fundamental principles of physics, and the underlying processes have unleashed new avenues of research in different areas [4–6]. The optical pumping of the atoms to a desired atomic state using the light field has been a widely used tool since its inception for functioning/improving the performance of atomic devices [7]. Generally, the performance of an atomic device scales as [8]

$$\frac{1}{\sqrt{NTt}}, \tag{1}$$

where the term T is transverse relaxation time, t is measurement time, and N is the fraction of atoms contributing to the signal. In an ideal situation, the N is desired to be the total number of atoms. However, the partial spectral overlap of the light field with the atomic ensemble and the atomic population in irrelevant states limits N. This partial overlap can be an issue while working with anti-relaxation-coated cells where a narrow linewidth laser can only couple with atoms of a particular velocity group. For a buffer gas-filled cell, most of the atoms can be coupled to the light field as the collisional homogeneous width is typically larger than the inhomogeneous Doppler broadening.

However, the atoms in the irrelevant states are a concern for both anti-relaxation-coated and buffer gas-filled cells. Hence, developing a suitable methodology to access these remaining atoms (not contributing to producing resonance signals) is quite important for efficiently working the atomic devices. In many instances, a repump laser is used to populate the desired atomic level [9,10], which effectively increases the amplitude of the resonance signal. However, it brings additional complexities and has a limited role in populating desired Zeeman states of the atomic level.

On the other hand, the coherent population trapping (CPT) based systems are immune to any population loss

(a)E-mail: spradhan@barc.gov.in (corresponding author)

as both hyperfine ground states of an atom are simultaneously coupled to a common excited-state using a bi-chromatic laser field [5,11–14]. In these systems, the amplitude of the CPT resonances is optimized by transferring the population to the desired Zeeman sublevels via manipulating the laser polarization and the direction of the applied magnetic field [15,16]. For example, Cox *et al.* [14] showed the possibility of building a vector magnetometer by measuring the relative amplitude of multiple CPT resonances at different magnetic field orientations using a linearly polarized bichromatic laser field. Similarly, several other groups have used the two-photon CPT resonances to build scalar atomic magnetometers to measure a longitudinal magnetic field applied parallel to the light propagation direction [5,17–20]. Careful application of an orthogonal magnetic field (*i.e.*, perpendicular to the light propagation direction) along with a longitudinal magnetic field can lead to very interesting population dynamics among ground-state Zeeman sublevels of a CPT-based system, and its implementation for enhanced magnetometry has not been explored in the past.

In this article, we show the efficient accumulation of population in relevant Zeeman states by using a circularly polarized bi-chromatic light field in combination with longitudinal and orthogonal magnetic fields. The prolonged interaction of the atoms with the light field in buffer gas is used to its advantage of rapid optical pumping. But most importantly, the Zeeman sublevels with the maximum population contribute to the form desired CPT resonance, resulting in a phenomenal increase in its amplitude (around 7-fold) under this combined action. This amplitude increase will help in improving the sensitivity for the magnetic field measurement. In addition, the envisaged methodology is suitable for the compact operation of the device [21].

The paper is organized with a brief description of the experimental apparatus. The amplitude of the CPT resonances for various combinations of the longitudinal and transverse magnetic fields is shown. A discussion on the utilized theoretical framework based on the semi-classical density matrix approach is presented. A comparison between the experimental and calculated signal profile with a reason for the deviation is discussed. The underlying physical process leading to enhanced optical pumping is described. In addition, we have discussed the role of Rabi frequency and ground-state relaxation rate in optimizing the strength of the CPT resonance.

Figure 1 shows the schematics of the experimental setup and the relevant atomic energy level used to produce the coherent population trapping (CPT) resonances with a bi-chromatic light. The experiment is performed on rubidium (Rb) atoms (natural isotopic composition) with N_2 gas at 25 torr in a glass cell (50 mm length and 25 mm diameter) at 48 °C. The vapor cell is mounted at the center of a four-layer magnetic shield, which is used to reduce the ambient magnetic field. A three-axis Helmholtz coils setup was installed inside the shield to apply bias

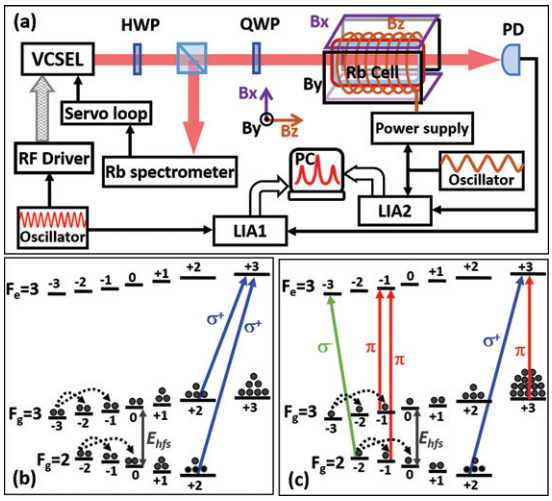

Fig. 1: (a) Schematic diagram showing essential components of the experimental setup. Energy level diagram showing (b) the σ^+ transitions in the presence of longitudinal magnetic field B_z, and in (c), the σ^+ and π transitions when both $B_z \neq 0$, $B_y \neq 0$. The stretched CPT resonance is formed by ($|F_g = 2, m_F = +2\rangle$, $|F_g = 3, m_F = +3\rangle$) coupled with blue and red solid lines. The green σ^- arrow also participate in many CPT manifolds but it is not shown due its feeble strength.

magnetic fields in all three directions. A Vertical Cavity Surface Emitting Laser (VCSEL) at 795 nm, 60 μW power with beam diameter 4.5 mm is frequency modulated by a radio frequency (RF) oscillator at 1.517866 GHz to generate sideband beams resonant from both ground states of ^{85}Rb to a common excited state $F_e = 3$ in D1 line. The RF oscillator is modulated at a frequency 440 Hz with a modulation of depth of 12 kHz. We consider the propagation direction of the laser beam along the z-axis. Using a quarter wave plate (QWP) before the vapor cell, the light polarization is set to circular. The light transmitted through the atomic sample is demodulated using a lock-in amplifier (LIA1) at the modulation frequency applied to the RF oscillator. Two-photon CPT resonances are observed by scanning the RF oscillator as the frequency difference ($\Delta\omega$) between the side mode of the laser beam matches with the separation between the ground Zeeman states (E_{hfs}) that are simultaneously coupled to an excited level Zeeman state of ^{85}Rb, as shown in fig. 1(b). Multiple Λ-systems are formed at different values of two-photon detuning defined as $\Delta = \Delta\omega - E_{hfs}$. Consequently, the magnetic field insensitive clock transition is observed at $\Delta = 0$ and magnetic field sensitive transitions at $\Delta \neq 0$.

We consider the propagation direction of the light field as the axis of quantization (*i.e.*, z-axis). The degeneracy in the hyperfine Zeeman sublevels is lifted by applying a longitudinal magnetic field B_z. Since the laser beam is circularly polarized, only σ^+ transitions are possible in the presence of B_z field (fig. 1(b)). The presence of any orthogonal magnetic field (B_x or B_y) leads to population redistribution among the Zeeman states, which can

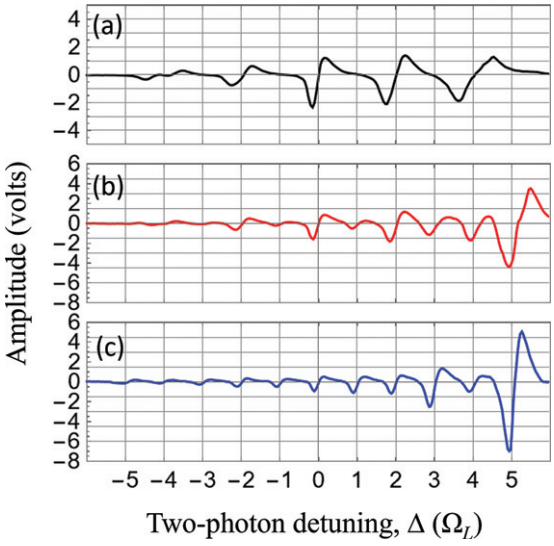

Fig. 2: Experimentally measured CPT resonances, with a dispersion lineshape produced through demodulation with respect to the modulation given to the RF field, as a function of two-photon detuning for different B_z and B_y values. (a) B_z = 51.7 mG, $B_y = 0$, (b) $B_z = 51.7$ mG, $B_y = 27.0$ mG, (c) B_z = 51.7 mG, $B_y = 48.5$ mG. In each plot, two-photon detuning (*i.e.*, x-axis) is normalized by dividing it by the Larmor frequency corresponding to the total applied magnetic field. All the signals were measured at a fixed gain of the lock-in amplifier (LIA1).

be understood in terms of additional π and σ transitions, as shown in fig. 1(c).

Figure 2 shows the experimentally measured profiles of the CPT resonance signal as a function of two-photon detuning (Δ) for different values of B_z and B_y fields. The CPT resoances are observed for multiple Δ values, *i.e.*, $\Delta = 0, \pm\Omega_L, \pm2\Omega_L, \pm3\Omega_L, \pm4\Omega_L, \pm5\Omega_L$, where the term $\Omega_L = g_F\mu_B B$ is the Larmor frequency corresponding to total applied field $B = \sqrt{B_z^2 + B_y^2}$, the μ_B is the Bohr magneton, and the g_F represents the gyromagnetic factors of the ground states of the ^{85}Rb atom. The both ground states $F_g = 2$ and $F_g = 3$ have the same magnitude of g_F factor but opposite sign. The CPT signal, obtained from the lock-in amplifier(LIA1) with respect to the modulation applied to the RF oscillator, exhibits a dispersive line profile [22]. In fig. 2, the linewidth of CPT resonances is limited by the modulation depth to the RF oscillator.

When a longitudinal magnetic field $B_z = 51.7$ mG is applied (fig. 2(a)), the five CPT resonances are observed at Δ values that are even multiples of Larmor frequency Ω_L, *i.e.*, $\pm4\Omega_L$, $\pm2\Omega_L$, 0. This is due to the presence of pure σ^+ polarization components in the bichromatic laser beam [14,16]. For this case, as shown in fig. 1(b), the σ^+ polarization components can only couple the Zeeman sublevels of the ground states having same value of m_F, resulting the different Λ systems responsible for producing CPT peaks. For each Λ system, the total energy shift between two sublevels is even multiples of Ω_L, which matches to Δ at CPT peak position.

Here, it should be noted that the stretched Zeeman state ($|F_g = 3, m_F = +3\rangle$) (fig. 1(b)) does not contribute to forming any CPT resonance. It is a major limitation for improving the sensitivity of the CPT-based atomic magnetometers as a majority population is trapped in the state ($|F_g = 3, m_F = +3\rangle$). Thus, the advantage of optical pumping using circularly polarized light is not fully utilized for magnetometry applications. As shown in fig. 1(c), the presence of a bias transverse magnetic field B_y (or B_x) generates π and σ transitions [11]. Thus, six additional ($\pm5\Omega_L$, $\pm3\Omega_L$, $\pm\Omega_L$) resonances appear in the spectrum when a small transverse field $B_y = 27.0$ mG is applied with $B_z = 51.7$ mG (fig. 2(b)), which are similar to resonances shown in ref [15,23] for ^{87}Rb in D1 line. As the strength of B_y gets close to B_z, the stretched $+5\Omega_L$ resonance coupled to ($|F_g = 3, m_F = +3\rangle$, $|F_g = 2, m_F = +2\rangle$) shows maximum amplitude due to larger population in these states, as shown in fig. 2(c). This indicates that the optical pumping to the stretched states and coupling them to the CPT manifold is possible with a circularly polarized light by changing the direction of the magnetic field, which was not observed experimentally in earlier report [23]. The amplitude of the $+5\Omega_L$ resonance increases by 8.3 times as the ratio of B_y/B_z value changes from 0.2 to 0.93. This rate of change of amplitude also depends on the laser beam intensity.

The sensitivity of a resonance to the change in magnetic field, apart from its amplitude and width, is a primary attribute for efficient use in magnetometry. The signal is usually obtained in a degenerate two-level system for near zero-field measurements by demodulating the light intensity with respect to a slowly varying magnetic field [6,24]. Figure 3 shows the spectral profile obtained through magnetic field demodulation for non-degenerate levels. A modulation amplitude of 160 nT at 55 Hz is added to the bias B_z field. The photo-diode signal is detected with a lock-in amplifier (LIA2) triggered to the magnetic modulation, as shown in fig. 1. The magnetically insensitive resonance at zero Ω_L frequency, corresponding to ($|F_g = 3, m_F = 0\rangle$, $|F_g = 2, m_F = 0\rangle$) coupling is not observed for any combination of magnetic field (fig. 3). This is because the modulation applied to the magnetic field does not affect the Zeeman states with $m_F = 0$.

Similarly to fig. 2, the stretched $+5\Omega_L$ resonance shows a progressive increase in its amplitude with B_y magnetic field, which is around seven times higher compared to $+4\Omega_L$ resonance shown in fig. 3(a). The $+4\Omega_L$ resonance is typically used to measure longitudinal magnetic fields [14]. The increase in the amplitude of $+5\Omega_L$ resonance with B_y field is consistent with the results shown in fig. 2. For $B_y \approx B_z$, unlike fig. 2(c), almost no resonance signals are observed at Larmor's frequencies $+4\Omega_L$, $+3\Omega_L$, $+2\Omega_L$, $+\Omega_L$ in fig. 3(c). Hence, the relative amplitude of the $+5\Omega_L$ resonance in fig. 3(c) is significantly higher. This behavior can be understood by

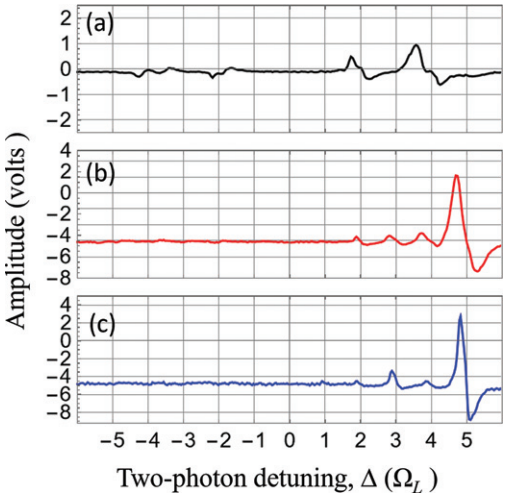

Fig. 3: Experimentally measured CPT resonances, with a dispersion lineshape produced through demodulation with respect to the modulation given to the magnetic field B_z, as a function of two-photon detuning for different B_z and B_y values. (a) $B_z = 51.7\,\text{mG}$, $B_y = 0$, (b) $B_z = 51.7\,\text{mG}$, $B_y = 27.0\,\text{mG}$, (c) $B_z = 51.7\,\text{mG}$, $B_y = 48.5\,\text{mG}$. All the signals were measured at a fixed gain of the lock-in amplifier (LIA2), which was the same as for the signals shown in fig. 2.

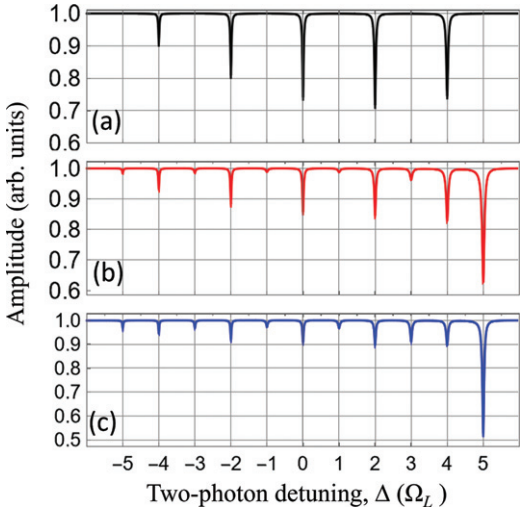

Fig. 4: Calculated CPT resonances as a function of two-photon detuning for different B_z and B_y values. (a) $B_z = 51.7\,\text{mG}$, $B_y = 0$, (b) $B_z = 51.7\,\text{mG}$, $B_y = 27.0\,\text{mG}$, (c) $B_z = 51.7\,\text{mG}$, $B_y = 48.5\,\text{mG}$. The parameters used in simulations are as follows: Rabi frequency $\Omega_R = 2\pi \times 150\,\text{kHz}$, and the ground-state relaxation rate $\gamma = 2\pi \times 100\,\text{Hz}$.

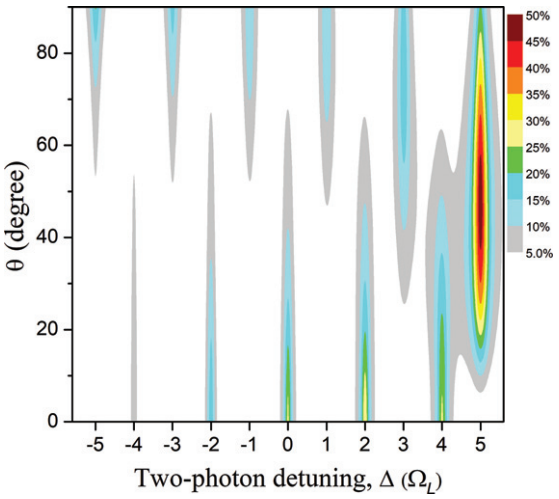

Fig. 5: Normalized amplitude of the CPT resonances as a function of two-photon detuning at different B_z and B_y fields by keeping total field $B = 11\,\text{mG}$. The percentage of individual signal amplitude is calculated with respect to the cumulative amplitude of all the resonances. The parameters used in simulations are as follows: Rabi frequency $\Omega_R = 2\pi \times 150\,\text{kHz}$, and the ground-state relaxation rate $\gamma = 2\pi \times 100\,\text{Hz}$.

considering that the Zeeman states ($|F_g = 3, m_F = +3\rangle$ and $|F_g = 2, m_F = +2\rangle$) responsible for producing the $+5\Omega_L$ resonance are most sensitive to the magnetic fields used in fig. 3. For example, the $5\Omega_L$ resonance will be 5/4 times more sensitive to the applied magnetic field than the conventionally used $4\Omega_L$ resonance. These attributes make $+5\Omega_L$ resonance an ideal candidate for magnetometry applications.

To understand our experimental observations of two-photon CPT resonances, we develop a theoretical model based on density matrix calculations for a three-level atom with Zeeman substates corresponding to realistic Rb atom [15]. Excitation of atoms via two light fields resonant from $F_g = 2$ and $F_g = 3$ to a common excited state $F_e = 3$ is considered in the presence of B_z and B_y magnetic fields. The optical Bloch equations obtained from the Liouville equation are numerically solved under the steady state conditions to calculate the light absorption through the medium. We have simplified our theoretical model by not considering the effect of buffer gas collisions and thermal averaging due to the motion of atoms. Figure 4 shows the theoretically calculated CPT resonances obtained using a continuous-wave (CW) bi-chromatic light beam with circular polarization at different B_z and B_y values. Positions and relative amplitude of theoretically calculated CPT resonances match very well with experimental observations shown in fig. 2. Particularly, the stretched $+5\Omega_L$ resonance shows the enhanced amplitude for $B_z \approx B_y$ in both the experiment (fig. 2(c) and fig. 3(c)) and theory (fig. 4(c)).

Figure 5 shows the 2D contour plot of the amplitude of all possible CPT resonances at different values of B_z and B_y while keeping the total magnetic field B ($= 11\,\text{mG}$) constant. Here, the strength of applied magnetic fields B_z and B_y is equal to $B\cos\theta$ and $B\sin\theta$, respectively. The angle θ is varied from 0° to 90° to change the B_z and B_y fields. The amplitude of each CPT resonance is normalized with respect to the total amplitude of all the resonances.

In fig. 5, in the presence of a longitudinal magnetic field B_z at $\theta = 0°$, strong CPT resonances at $+4\Omega_L$, $+2\Omega_L$, and 0 are observed, which matches with the signal shown

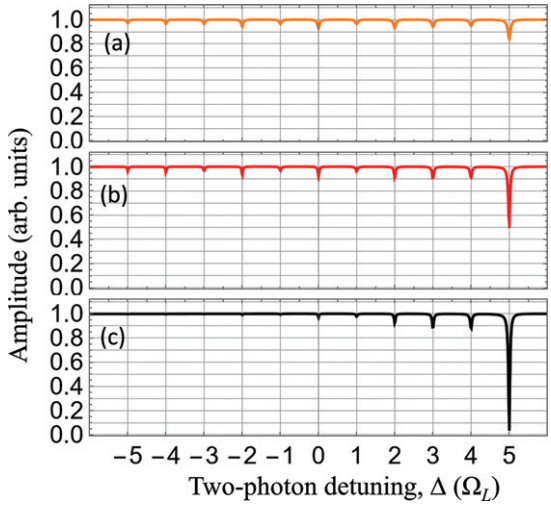

Fig. 6: Calculated CPT resonances as a function of two-photon detuning for different ground-state relaxation rates γ at fixed values of $B_z = 51.7\,\text{mG}$, and $B_y = 53.8\,\text{mG}$. (a) $\gamma = 2\pi \times 500\,\text{Hz}$, (b) $\gamma = 2\pi \times 100\,\text{Hz}$, and (c) $\gamma = 2\pi \times 1\,\text{Hz}$. The amplitude of each plot is normalized. In each plot, two-photon detuning (*i.e.*, x-axis) is normalized by dividing it by the Larmor frequency corresponding to the total applied magnetic field

in fig. 2(a). However, as the angle θ is increased from zero, the strength of the transverse magnetic field B_y increases, and the amplitude of resonances at even integer multiples of Ω_L reduces. On the other hand, the amplitude of $+5\Omega_L$ resonance enhances significantly, and it becomes maximum when $B_y \approx B_z$ around $\theta = 45°$. A significant decrease in the relative amplitude of other resonances at $B_y \approx B_z$ clearly indicates the enhanced Zeeman optical pumping to the stretch Zeeman states $|F_g = 3, m_F = +3\rangle$ and $|F_g = 2, m_F = +2\rangle$. As the strength of field B_y is further increased (*i.e.*, for angle $\theta > 45°$), the $+5\Omega_L$ resonance gets weak. The amplitude of other CPT resonances positioned at odd integer multiples of Ω_L, including $-5\Omega_L$, $\pm 3\Omega_L$, $\pm\Omega_L$, starts to increase. For angle θ above 70°, the CPT resonances at even integer multiples of Ω_L vanishes completely, as seen in fig. 5.

As we can see in fig. 4(c), for $B_z \approx B_y$, the $+5\Omega_L$ resonance accounts for around 50% of the total strength of the CPT resonances at $\Omega_R = 2\pi \times 150\,\text{kHz}$, and $\gamma = 2\pi \times 100\,\text{Hz}$. This strength can be further improved by adjusting the Ω_R and γ values. Figure 6 shows the theoretically calculated CPT resonances as a function of two-photon detuning for different values of ground-state relaxation rate γ when the fields $B_z \approx B_y$. Here, by keeping Ω_R fixed, the ground-state relaxation rate is lowered from 500 Hz to 1 Hz, which significantly enhances the amplitude of $+5\Omega_L$ resonance. For relaxation rate $\gamma = 2\pi \times 1\,\text{Hz}$, the $+5\Omega_L$ resonance has more than 80% of the total strength of the CPT resonances (fig. 6(c)). Such low relaxation rate can be realized with anti-relaxation-coated cell or laser-cooled atoms.

The $+5\Omega_L$ resonance is highly sensitive to the magnetic field and is an ideal candidate for performing magnetometry. Further, in this configuration, the state $|F_g = 3, m_F = +3\rangle$ is coupled by a π transition, as shown in fig. 1(c). There will also be a weaker coupling by the σ^- transition due to a smaller relative transition amplitude. The disparity in the transition strength has been used in the literature to enhance the relevant signal amplitude in pump-probe spectroscopy [25]. Since the π and intrinsically strong σ^+ transition (as the light field is σ^+ polarized) are part of the CPT manifold, the single-photon excitation process through σ^- transition is hampered, and pumping back from $|F_g = 3, m_F = +3\rangle$ is reduced. This makes the population trapping in the stretched state even more robust. Importantly, the phenomenon opens an interesting way to control the optical pumping by manipulating the magnetic field and will be useful for quantum state engineering required for various applications [26,27].

In conclusion, a complementary method to use inaccessible atomic populations for magnetometry applications is explored. Using a circularly polarized bichromatic light field, we demonstrated that a specific combination of longitudinal and transverse magnetic fields shows a remarkable increase in the strength of the stretched CPT resonance. It provides an interesting approach to transfer the population to the stretch state by playing with the magnetic field and fully utilizing the population without compromising on the requirement for compact operation of the device. The fundamentals of the associated physical processes will be useful in quantum technology relying on coherent manipulation of atomic dynamics using light and magnetic fields. Our experimental observation is consistent with the theoretical calculation based on the density matrix approach.

* * *

The authors are thankful to Dr. D. V. Udupa for facilitating their work.

Data availability statement: The data that support the findings of this study are available upon reasonable request from the authors.

REFERENCES

[1] Wu X., Liang X., Tian Y., Yang F., Chen C., Liu Y.-C., Tey M. K. and You L., *Chin. Phys. B*, **30** (2021) 020305.
[2] Lin G.-W., Zou X.-B., Lin X.-M. and Guo G.-C., *Phys. Rev. A*, **79** (2009) 042332.
[3] Aslam N., Zhou H., Urbach E. K., Turner M. J., Walsworth R. L., Lukin M. D. and Park H., *Nat. Rev. Phys.*, **5** (2023) 157.
[4] Budker D., Kimball D., Rochester S., Yashchuk V. and Zolotorev M., *Phys. Rev. A*, **62** (2000) 043403.

[5] Knappe S., Shah V., Schwindt P. D., Hollberg L., Kitching J., Liew L.-A. and Moreland J., *Appl. Phys. Lett.*, **85** (2004) 1460.
[6] Pradhan S., *Rev. Sci. Instrum.*, **87** (2016) 093105.
[7] Kastler A., *Science*, **158** (1967) 214.
[8] Budker D. and Romalis M., *Nat. Phys.*, **3** (2007) 227.
[9] Zhang R., Kanta D., Wickenbrock A., Guo H. and Budker D., *Phys. Rev. Lett.*, **130** (2023) 153601.
[10] Chowdhury S. R. and Pradhan S., *J. Phys. B: At. Mol. Opt. Phys.*, **55** (2022) 165502.
[11] Wynands R., Nagel A., Brandt S., Meschede D. and Weis A., *Phys. Rev. A*, **58** (1998) 196.
[12] Knappe S., Schwindt P. D., Shah V., Hollberg L., Kitching J., Liew L.-A. and Moreland J., *Appl. Phys. Lett.*, **13** (2005) 1249.
[13] Yudin V. I., Taichenachev A. V., Dudin Y. O., Velichansky V. L., Zibrov A. S. and Zibrov S. A., *Phys. Rev. A*, **82** (2010) 033807.
[14] Cox K., Yudin V. I., Taichenachev A. V., Novikova I. and Mikhailov E. E., *Phys. Rev. A*, **83** (2011) 015801.
[15] Margalit L., Rosenbluh M. and Wilson-Gordon A. D., *Phys. Rev. A*, **88** (2013) 023827.
[16] Warren Z., Shahriar M. S., Tripathi R. and Pati G. S., *Metrologia*, **54** (2017) 418.
[17] Shah V., Knappe S., Schwindt P. D. and Kitching J., *Nat. Photon.*, **1** (2007) 649.
[18] Pradhan S., Kani A., Wanare H., Mishra S. and Das A. K., *J. Phys. B: At. Mol. Opt. Phys.*, **48** (2015) 075502.
[19] Xu C., Wang S.-G., Hu Y., Feng Y.-Y. and Wang L.-J., *Chin. Phys. B*, **26** (2017) 064203.
[20] Hong H.-G., Park S. E., Lee S.-B., Heo M.-S., Park J., Kim T. H., Kim H. Y. and Kwon T. Y., *Sensors*, **21** (2021) 1517.
[21] Schwindt P. D. D., Knappe S., Shah V., Hollberg L., Kitching J., Liew L.-A. and Moreland J., *Appl. Phys. Lett.*, **85** (2004) 6409.
[22] Pradhan S., Kani A., Wanare H., Behera R. and Das A., *Phys. Rev. A*, **85** (2012) 063805.
[23] Pati G. S., Tripathi R., Grewal R. S., Pulido M. and Depto R. A., *Phys. Rev. A*, **104** (2021) 033116.
[24] Seltzer S. J. and Romalis M. V., *Appl. Phys. Lett.*, **85** (2004) 4804.
[25] Pradhan S. and Jagatap B. N., *J. Opt. Soc. Am. B*, **28** (2011) 398.
[26] Finkelstein R., Lahad O., Cohen I., Davidson O., Kiriati S., Poem E. and Firstenberg O., *Phys. Rev. X*, **11** (2021) 011008.
[27] Main D., Hird T. M., Gao S., Oguz E., Saunders D. J., Walmsley I. A. and Ledingham P. M., *Phys. Rev. A*, **103** (2021) 043105.